JOURNAL OF PLANKTON RESEARCH | VOLUME 32 | NUMBER 4 | PAGES 515–527 | 2010

An algal photoprotection index and vertical mixing in the Southern Ocean

GARY P. GRIFFITH[1]*, ROSS VENNELL[1] AND MICHAEL J. M. WILLIAMS[2]

[1]DEPARTMENT OF MARINE SCIENCE, OTAGO UNIVERSITY, 310 CASTLE STREET, DUNEDIN 9054, NEW ZEALAND AND [2]DEPARTMENT OF MARINE PHYSICS, NATIONAL INSTITUTE OF WATER AND ATMOSPHERE, PO BOX 14901 KILBIRNIE, WELLINGTON 6022, NEW ZEALAND

*CORRESPONDING AUTHOR: gary.griffith@otago.ac.nz

Received September 3, 2009; accepted in principle December 10, 2009; accepted for publication January 3, 2010

Corresponding editor: William K.W. Li

We explored the relationship between mixing dynamics in the surface mixed layer and the photoprotective response of phytoplankton. The distribution of photoprotective pigments was determined at 15 stations in subantarctic waters southeast of New Zealand during austral autumn. The first-order kinetics of the phytoplankton photoprotective response to both light and dark was determined using *in situ* simulated (deck) incubations. The vertical mixing regime was deduced from two physical parameterizations based on CTD and ADCP profiles. A photophysiological index based on the vertical profile of de-epoxidation state (DES) of the diadinoxanthin-cycle to changes in light intensity was compared with the two physical estimates of vertical eddy diffusivity. For short time scales (<12 h) and within a similar water mass, the DES index provides within one order of magnitude an estimate of average vertical velocity representative of the bulk vertical eddy diffusivity. From the results, a conceptual model is presented of the quantitative relationship between vertical mixing and phytoplankton photoprotection in the water column. This relationship can provide additional insights into the effects of changes in vertical eddy diffusivity in the surface mixed layer on the photoprotective response of phytoplankton.

KEYWORDS: diadinoxanthin cycle; vertical mixing; photoprotection; Southern Ocean

INTRODUCTION

Understanding the relationship between vertical mixing and phytoplankton photoacclimation has been a major goal for oceanographers (Dusenberry *et al.*, 1999). Theoretical models suggest that the distribution and variance of photoacclimation properties within a population of cells are related to the mixing dynamics (Falkowski, 1983; Cullen and Lewis, 1988; Dusenberry, 2000). The underlying theory assumes that if the water column is perfectly stable and the surface irradiance constant, light-dependant physiological processes will adjust to the ambient light at that depth. Any vertical mixing would disturb this ideal photoacclimation. Indices of different physiological responses to light will readjust to light at different rates and on different time scales. The vertical distribution of the photophysiological indices with depth will provide information on the light history of the phytoplankton and can be used to estimate the vertical mixing rate. This concept has been applied to field studies using a range of physiological indices including single-cell fluorescence (Therriault *et al.*, 1990; Dusenberry *et al.*, 1999; Dusenberry, 2000), photosynthesis–irradiance relationships (Franks and Marra, 1994), carbon to chlorophyll ratios (Cullen and Lewis, 1988), enzyme activity (MacIntyre and Geider, 1996) and variable fluorescence (Oliver *et al.*, 2003).

doi:10.1093/plankt/fbq003, available online at www.plankt.oxfordjournals.org. Advance Access publication February 1, 2010

Several studies have investigated the time scales of mixing in offshore marine ecosystems using photophysiological indices based on the photoprotective response of algal cells via the carotenoid pigments changes associated with the xanthophyll cycle (XC) (Bidigare *et al.*, 1987; Olaizola *et al.*, 1992; Kashino *et al.*, 2002; Brunet *et al.*, 2006, 2007, 2008). In several algal classes including Bacillariophyta (diatoms), Dinophyta (dinoflagellates), Haptophyta and some Chrysophyta which together are largely responsible for oceanic primary production, the photoprotective response is through an enzyme controlled de-epoxidation of diadinoxanthin (Dd) to diatoxanthin (Dt) which dissipates excess light energy into heat to protect the photosynthetic machinery of photosystem II (Casper-Lindley and Bjorkman, 1998; Lavaud *et al*, 2004; Dimier *et al.*, 2007).

The de-epoxidation state (DES) is activated with increasing irradiance resulting in the rapid interconversion of Dd to Dt (seconds to minutes) (Arsalane *et al.*, 1994; Olaizola and Yamamoto, 1994). Under sustained or intermittent high irradiance, there is a gradual increase in the pool of Dd-cycle pigments (minutes–hours) (Olaizola and Yamamoto, 1994; Olaizola *et al.*, 1994; Fujiki and Taguchi, 2002; Lavaud *et al.*, 2002a, b, 2007). Under dark or very low light conditions, the reverse and slower interconversion of the pigments occurs with the epoxidation (ES) of Dt to Dd.

XC activity is also a function of other variables apart from light. The cellular content of Dd varies with species (Jeffrey and Vesk., 1997). Apart from diatoms, the ecophysiology of the XC cycle has been compared in pico- and nano-phytoplankton species demonstrating a large diversity in XC activity and efficiency possibly related to the ecological characteristics (Dimier *et al.*, 2009a, b). Algal XC activity is also dependant on the physiological and nutritional state of the algae (Staehr *et al.*, 2002). The cellular content of XC pigments has been observed to increase in stressed phytoplankton without any change in light conditions (Brunet *et al.*, 1996, Staehr *et al.*, 2002). Low iron concentrations result in higher content of Dd per unit of Chl *a* (Kosakowska *et al.*, 2004).

Studies on the relationship between vertical mixing and XC activity have employed different photophysiological indices including Dd/Chl *a*, Dt/Chl *a*, (Dd + Dt)/Chl *a* and Dt/(Dd + Dt). Each of these indices potentially represents a different time scale of photoprotection. Using the ratio Dd/Chl *a*, Claustre *et al.* (Claustre *et al.*, 1994) successfully determined vertical velocities at a geostrophic front in the Alboran Sea, whereas the ratio (Dd + Dt)/Chl *a* provided estimates of vertical displacement rates and turnover times during the development of a large Antarctic diatom bloom (Moline, 1998). By incorporating Dd, both these indices imply long-term processes (days–weeks). The reliability of photophysiological indicators incorporating Chl *a* as an indicator of biomass and physiological status has been questioned (Kruskopf and Flynn, 2006). The use of indices with normalization by Chl *a* is considered misleading as it includes algal biomass without Dd-cycle pigments (Brunet *et al.*, 2007). Studies in the Mediterranean Sea have shown the value of the DES index Dt/(Dd + Dt) rather than Dt/Chl *a* to realistically infer vertical mixing velocities (Brunet *et al.*, 2003, 2007, 2008).

The usefulness of this approach depends on reliable and independent physical estimates of the rate of vertical mixing. In typical ocean mixing events, the vertical length scale of motion mixing is small (order of cm), consequently it has been very difficult to obtain estimates of vertical mixing in the surface mixed layer by physical means (Cisewski *et al.*, 2005). Indirectly, vertical mixing can be estimated from parameterizations applied to conductivity, depth, temperature (CTD) data and Acoustic Doppler current profiler (ADCP) data.

The aim of this study is 3-fold: first, to compare the DES index to oceanographic conditions in subantarctic waters. Secondly, to obtain estimates of vertical mixing using two different physical parameterizations and compare these to the biological DES index. Thirdly, to develop a simple hypothetical model of the relationship between irradiance and the DES index which can provide information on vertical mixing.

METHOD

Sampling

This study was conducted as part of the National Institute of Water and Atmospheric Research (NIWA) cruise SAA5 in subantarctic waters south-east of New Zealand in Austral autumn between 26th of April 2003 and 27th of May 2003. Fifteen stations were sampled along two east–west transects (Fig. 1).

Profiles of temperature, salinity and density were collected with a CTD Sea-Bird 911*plus* profiler with an attached 12-bottle water sampler. A dual sensor configuration was employed (two conductivity sensors and two temperature sensors) together with oxygen and altimeter sensors. Photosynthetically active radiation (PAR) 400–700 nm was measured using a Biospherical Instruments QSP-2000 Quantum Scalar Sensor. The instruments were calibrated before and after the cruise. During the cruise, *in situ* calibration for temperature was carried out with reversing thermometers, and salinity

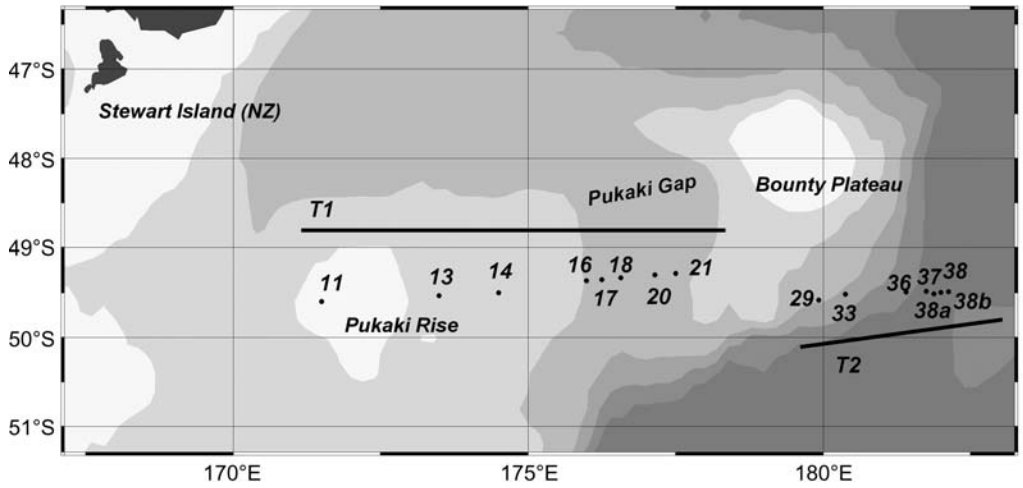

Fig. 1. Study site and sampling stations along transects T1 and T2.

samples were analysed with an Autosal Salinometer on board. Details of the processing and calibration of the temperature and salinity data are given in Walkington (Walkington, 2003). Temperature is estimated to be accurate to $\pm 0.002^{\circ}$C and salinity to ± 0.005 psu. The usual descent rate was 1.0 m s^{-1} corresponding to a vertical resolution of ± 4 cm with data sampling at 1 m intervals.

Current velocities were measured continuously along the ship's track with a hull mounted 150 kHz RD instruments ADCP. The ship's velocity was calculated from Global Positioning System (GPS) fixes. Due to the depth (up to 3000 m) at many of the stations, it was not possible to use the bottom tracking function of the ADCP to measure the ADCP's speed-over-bottom and detected range-to-bottom. The absolute heading, roll and pitch data from the ship's gyro platforms were used to convert the ADCP velocities into earth coordinates velocity by subtracting the ship's velocity from the relative water velocity measured by the ADCP. Only the ADCP data collected while the ship was stationary for CTD casts have been used. The data were collected in 4 m depth bins with the uppermost layer centred at 17 m depth to remove surface effects. The averaging interval was 300 s. The ADCP data were processed using MATLAB routines.

Estimation of the DES first-order rate constant

The first-order rate constant k (h^{-1}) was calculated for the DES index under natural light (deck incubations) for the shift in light intensity from dawn and for the reversal conversion for the ES index in the dark from sunset. Three on-board incubation experiments were conducted on clear sky days using water collected 2 h before dawn from the surface at the Campbell Plateau (Site 11), Pukaki Gap (Site 21) and the Bounty Plateau (Site 33). The samples were incubated on deck in three clear 20 L polycarbonate containers screened with Lee neutral density filters to allow 90% of incident light. All samples were placed in a bath of seawater fed from a deck hose, to keep the samples at the temperature (8–11°C) of the surrounding ocean. The samples were also slightly stirred for 30 s every 30 min to re-suspend any cells that may have settled. Triplicates samples for both the light and dark conversions were collected at regular intervals and were immediately filtered in the dark onto Whatman 25 mm GF/F glass-fibre filters, frozen by liquid nitrogen and stored in liquid nitrogen (−196°C) until analysis within 2 months. PAR was continually measured with a Li-Cor LI-192SA underwater quantum sensor attached to the bottom of one of the sampling containers exposed to daylight and connected to a Li-Cor Li-1000 datalogger.

The first-order rate constant k (h^{-1}) for the DES index in the light and the ES index in the dark was determined from the on-board incubation experiments by fitting the first-order kinetic model of Falkowski (Falkowski, 1983):

$$-k = \frac{1}{t}\ln\left(\frac{P_t - P_\infty}{P_0 - P_\infty}\right) \quad (1)$$

The rate constant is defined by the slope of the logarithmic progression of the DES index or ES index versus time t where $P = \mathrm{Dt}/(\mathrm{Dd} + \mathrm{Dt})$ or $\mathrm{Dd}/(\mathrm{Dd} + \mathrm{Dt})$. P_t is the ratio at time t, P_0 is the ratio at time zero and P_∞ is the ratio when cells become acclimated to the ambient light.

Phytoplankton collection and pigment analysis

At each sampling station (Fig. 1), discrete water samples were collected at 10-m intervals to 50 m using 10 L Niskin bottles mounted on the CTD rosette sampler. Surface samples were also collected at the same time. Water samples were initially pre-screened through a 200 μm nylon mesh net to remove large zooplankton and debris. Two litre samples were immediately filtered in the dark onto Whatman 25 mm GF/F glass-fibre filters, frozen by liquid nitrogen and stored in liquid nitrogen (−196°C) until analysis within 2 months. Storage under liquid nitrogen results in the recovery of at least 96% of pigments after 1 year (Mantoura *et al*, 1997). To extract the pigments, the filters were cut into small pieces and placed in 2.5 mL micro centrifuge tubes with 100% methanol. The samples were placed in an ice bath and sonicated in the dark for 15 min. The samples remained in the dark and were extracted at −20°C for 24 h. After extraction, the samples were centrifuged to remove the filter paper and then filtered through a 0.45 μm PTFE filter. The samples were then analysed by high performance liquid chromatography using a Shimadzu LC-10AD with a SCL-10aVP system controller. Three replicates were processed for each sample ($n = 90$) and averaged. The pigments were separated using a Phenomenex Onyx Monolithic C8 column 100 × 4.6 mm. The pigments were separated using a carotenoid specific analytical gradient protocol (Zapata *et al*., 2000) with methanol:acetonitrile:aqueous pyridine (50:25:25 v:v:v) as Solvent A and acetonitrile: acetone (80:20 v:v) as solvent B at a flow rate of 0.8 mL over 40 min.

Just prior to the HPLC run, an ion pairing solution (1.0 M ammonium acetate) was added to each sample vial in a ratio of three part extract:one part ammonium acetate to improve peak resolution (Wright and Mantoura, 1997). The separated pigments were detected at 436 nm and identified using Shimadzu Class-VP version 5.032 software. Standard pigments of Dd, Dd and Chl *a* were purchased from DHI Water and Environment in Denmark and the concentration of each pigment was determined against these standards.

Estimation of the vertical velocities of the phytoplankton cells

Estimates of the vertical velocity of the phytoplankton cells from a depth of 50 m to the surface were determined from the model of Falkowski (Falkowski, 1983) based on first-order kinetics:

$$T_{PP} = \frac{1}{-k}\ln\left(\frac{P_t - P_\infty}{P_0 - P_\infty}\right) \quad (2)$$

where T_{PP} was the time for a pigment change within the water column under daylight for a phytoplankton cell transported from a depth of 50 m to the surface. P is the DES index, P_0 the DES index at 50 m depth and P_t is the DES index at the surface. P_∞ and the first-order rate constant k were calculated from the on-board incubation experiments.

The de-epoxidation first-order rate constant k for the DES index was adjusted to allow for the epoxidation in the dark of some of the Dt to Dd as the samples were returned to the surface and for the time of filtering (∼20 min per sample) using the epoxidation first-order rate constant k determined from the on-board incubation experiments. The vertical velocity (m s^{-1}) was then calculated by dividing the depth (50 m) by the time T_{PP}

Estimation of the vertical eddy diffusivity and other quantities from the physical data

From the CTD profiles, estimates of the Brunt Väisälä frequency squared N^2, which provides a measure of the vertical stratification or static stability of the water column was calculated according to:

$$N^2 = \left(\frac{g}{\rho 0}\right)\left(\frac{\Delta\rho}{\Delta z}\right) \quad (3)$$

where g is the acceleration due to gravity, $\rho 0$ is the reference density and $\Delta\rho/\Delta z$ is the density gradient over the depth interval Δz. The CTD data were sub-sampled at equivalent depth intervals to the ADCP data (4 m depth spacing). The squared shear S^2 was estimated from the ADCP data at 4 m depth intervals with the uppermost bin centred on the 17 m depth:

$$S^2 = \left(\frac{\partial u}{\partial z}\right)^2 + \left(\frac{\partial v}{\partial z}\right)^2 \quad (4)$$

where u and v are the two components of the horizontal velocity and z the depth bin.

Calculation of shear does not require ADCP measured absolute velocities.

An estimate of noise in the ADCP calculation is needed to assess the accuracy of Richardson number-based parameterizations. As these measurements were taken with the ship stationary, errors related to ship movement were small. Based on the manufacturer's specifications for the ADCP, a depth cell length of 4 m and

an ensemble length of 120 s, the short-term accuracy is ~ 0.5 cm s^{-1} producing an root mean square (RMS) error of $S^2 < 1 \times 10^{-6}$.

From the Brunt Väisälä squared $\mathcal{N}^2$ and the squared shear S^2, the vertically averaged gradient Richardson number Ri, which represents the ratio of the stabilizing stratification to the destabilizing shear, was obtained according to:

$$Ri = \frac{\mathcal{N}^2}{S^2} \tag{5}$$

The vertical diffusivity K_G associated with internal waves was derived using the parameterization of Gregg (Gregg, 1989):

$$K_g = 5 \times 10^{-6} \text{ m}^2 \text{ s}^{-1} \left\langle \frac{S^4}{\mathcal{N}^4} \right\rangle. \tag{6}$$

The coefficient (5×10^{-6}) has been applied so that the internal wave variance is consistent with the Garrett–Munk spectrum (Garrett and Munk, 1979).

The bulk vertical diffusivity K_{PP} was estimated using the equation of Pacanowski and Philander (Pacanowski and Philander, 1981):

$$K_{PP} = \frac{5 \times 10^{-3} \text{ m}^2 \text{ s}^{-1} + 10^{-4}(1 + 5Ri)^2}{(1 + 5Ri)^3} + 10^{-5} \tag{7}$$

RESULTS

Pigment distributions, light and hydrography

The pigment distribution of Dd/Chl *a* and Dt/Chl *a* showed significant spatial variation (Fig. 2). Dd/Chl *a* and Dt/Chl *a* were the highest at Station 11 on the Pukaki rise decreasing eastward across the Pukaki Gap. The ratios for both Dd/Chl *a* and Dt/Chl *a* were low on the edge of the Bounty Plateau at Stations 29 and 33. The highest ratio of Dt/Chl *a* occurred from the eastern edge of the Bounty Plateau across to Bollons Seamount between Stations 36 and 38.

Two different water types representing variations of Subantarctic Mode Water (SAMW) were identified in the surface mixed layer from the potential temperature, salinity and potential density profiles. Warm and salty water SAMW is present between Stations 11 and 14 and between Stations 36 and 38. Fresher and colder SAMW occurs in the Pukaki Gap between Stations 16 and 21. A detailed description of water masses in the region is provided in Morris *et al.* (2001).

The DES index and irradiance (Fig. 3) was significantly correlated (Pearson's correlation $r = 0.68$, $n = 31$). There was no correlation between temperature, salinity and potential density.

Vertical distribution of DES

The vertical distributions of the DES index from the surface to 50 m for all daytime stations are shown in Fig. 4. Due to operational constraints, it was only possible to sample to 50 m and not to the base of the surface mixed layer at all stations. The shape of the profiles varied significantly between stations. The shape of the profiles can be interpreted in terms of the Cullen and Lewis (Cullen and Lewis, 1988) logistic model. The distribution of the DES with depth is an indication of the relative magnitude of the short-term time scale (minutes to hours) of the photoprotective response of the phytoplankton relative to the time scale of mixing. The near vertical distribution of the index at Station 11 suggests that the rate of vertical mixing was faster than the photoprotective response of the phytoplankton. The exponential decrease with depth of the ratio at Station 29 implies that the rate of vertical mixing was slower than the photoprotective response. The depth profiles of the other stations represent a situation where the rate of vertical mixing and photoprotection varies through the profile. In the upper 20 m of Stations 13, 15, 18, 29 and 33, the photoprotective response was greater than for vertical mixing. Below 20 m, the magnitude of the photoprotective response was less but still greater than the rate of vertical mixing. At all the stations, the highest values for the index occurred near or at the surface.

On-board pigment kinetic experiments

The first-order kinetic coefficients (k, h^{-1}) from the three on-board time-course experiments for the change in the DES with increasing irradiance from dawn to 2 h after midday varied between 0.02 and 0.037 h^{-1} (Table I). The rate constants were similar for the three different deck incubation experiments although surface irradiance conditions varied. The P_∞ value (zero-order kinetics) varied between 0.3 and 0.38. The rate constants for the change in the ES in the dark were much slower and varied between 0.003 and 0.009 h^{-1}.

Estimated vertical velocities and mixing times from the DES index

Estimates of the vertical velocity (m s^{-1}) and mixing times (h^{-1}) of a phytoplankton cell determined from the DES are shown in Table II. The estimates were calculated using equation (2) with a rate constant k of

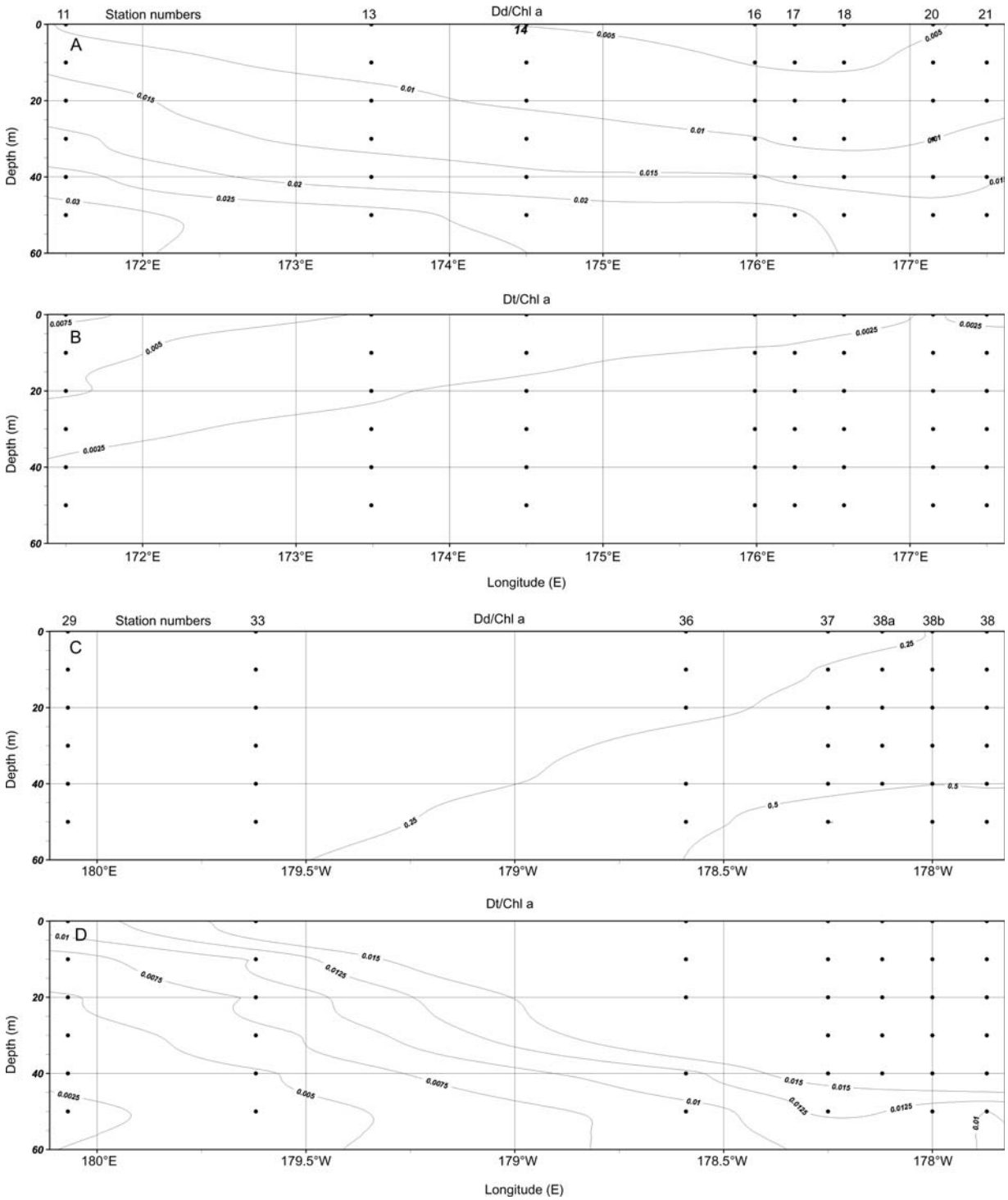

Fig. 2. Longitudinal distribution of the XC pigment concentrations (**A**), Dd/Chl *a* along transect T1 (**B**), Dt/Chl *a* along T1 (**C**), Dd/Chl *a* along transect T2 (**D**), Dt/Chl *a* along T2.

0.026 (h^{-1}), which represents the average from the three on-board incubations (Table I). The vertical velocities varied from 9.22×10^{-5} m s^{-1} at Station 36 to 1.05×10^{-3} m s^{-1} at Station 20. The estimated time of mixing within the upper 50 m lay between 7 h and 150 h.

Physical estimates of vertical mixing

Two different estimates of the vertically averaged eddy diffusivities were calculated from the ADCP and CTD data (Table II). The K_{PP} values are an estimate of bulk vertical diffusivity based on the parameterization given by Pacanowski and Philander (1981), whereas the K_G estimates derived from the parameterization given by Gregg (1989) are an estimate of the vertical diffusivity associated with internal waves. Parameterizations of vertical eddy diffusivity based only on the Brunt Väisälä frequency (N) do not take into account locally generated shear. The Richardson number Ri based parameterizations used in this study are a more appropriate function as they represent the balance between the stabilizing buoyancy frequency and the destabilizing shear (Law *et al.*, 2003). These estimates of bulk eddy diffusivity can be considered to be an integrated measure of all the mixing processes providing a "background" estimate of the physical processes transporting phytoplankton up and down within the euphotic zone. Vertical averages for K_{PP} within the upper 50 m ranged from 1.02×10^{-3} to 9.35×10^{-3}. Quantitatively, K_G was one to two orders of magnitude smaller than K_{PP} and ranged between 9.37×10^{-5} and 8.08×10^{-4}.

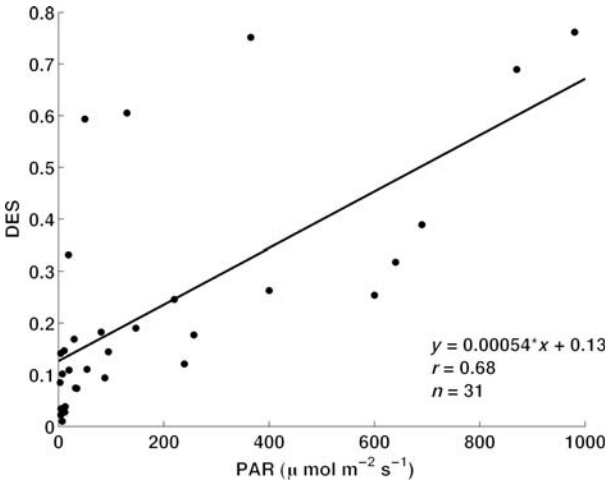

Fig. 3. Relationship between DES and PAR.

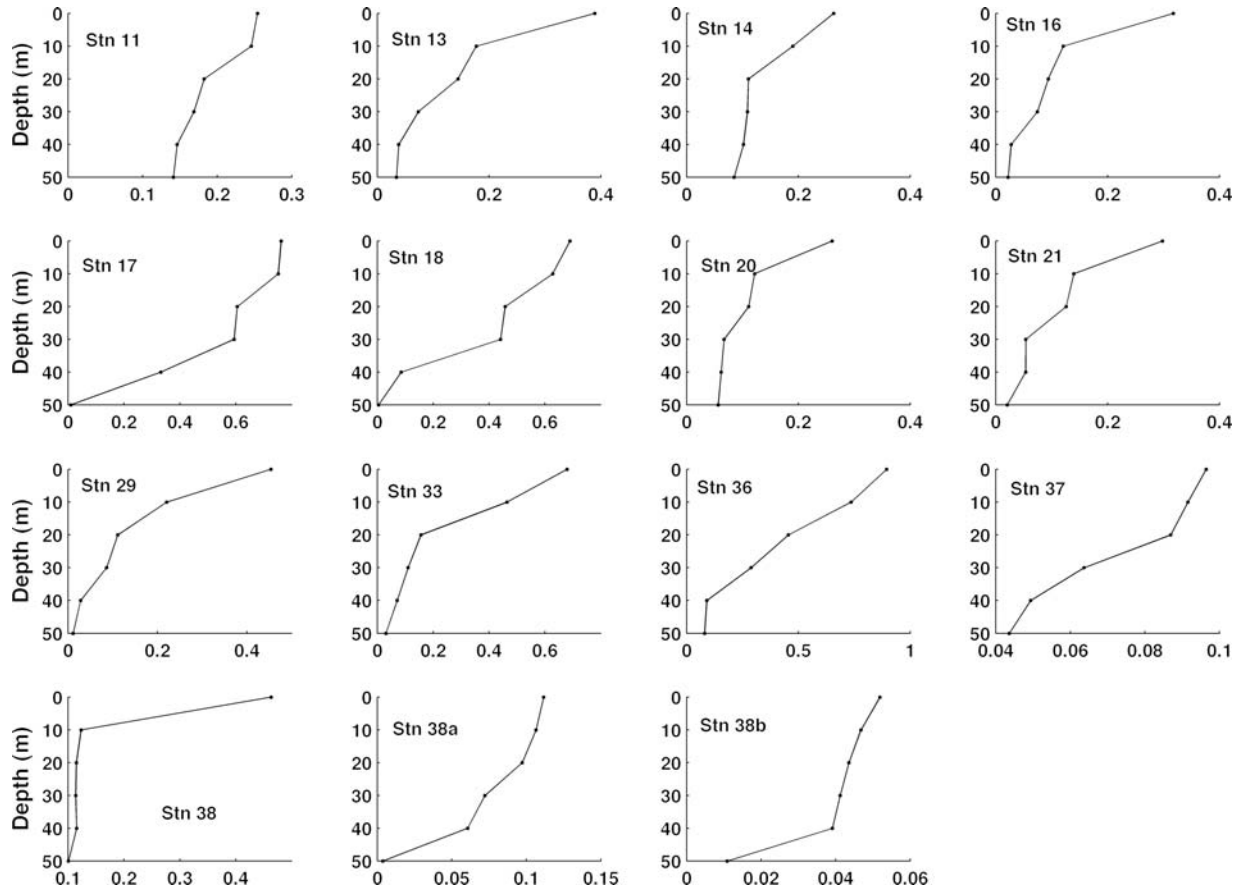

Fig. 4. Daytime vertical profiles of DES. Stn, sampling stations.

Table I: First-order kinetic coefficients (k, h^{-1}) for the DES [Dt/(Dd + Dt) ratio] under natural light from dawn to 2 h after midday the three on-board incubation experiments

Site	Light environment	DES k (h^{-1})
Campbell Plateau; Station 11 49.36.00°S, 171.30.05°E	LL to HL (11–600 μmol photons m^{-2} s^{-1})	0.025 ± 0.0017
Pukaki Gap; Station 21 49.17.06°S, 177.29.94°E	LL to HL (8–450 μmol photons m^{-2} s^{-1})	0.033 ± 0.0019
Bounty Plateau; Station 33 48.15.45°S, 179.29.93°E	LL to HL (45–900 μmol photons m^{-2} s^{-1})	0.02 ± 0.0035

Mean values with standard error of the mean ($n = 3$). P_∞, the final DES ratio at the end of the experiment.

Table II: Estimates of the DES derived vertical velocity ($m\ s^{-1}$) and mixing times (h^{-1}) and the vertically averaged eddy coefficients ($m^2\ s^{-1}$) for the physically derived parameterizations K_{PP} and K_G

Stn	Sampling start time (NZDT)	MLD (m)	DES vertical velocity ($m\ s^{-1}$)	DES mixing time (h^{-1})	K_{PP} ($m^2\ s^{-1}$)	K_{PP} MT (h^{-1})	K_G ($m^2\ s^{-1}$)	K_G MT (h^{-1})	VMI
11	12:30	102	1.80×10^{-3}	7.7	1.53×10^{-3}	9	4.66×10^{-4}	29.9	0.56
13	13:54	92	5.27×10^{-4}	26	1.17×10^{-3}	11.9	2.76×10^{-4}	50.5	0.19
14	10:00	74	1.18×10^{-3}	11.8	1.02×10^{-3}	13.6	2.15×10^{-4}	64.9	0.37
16	14:10	62	7.06×10^{-3}	2	4.92×10^{-3}	2.8	7.37×10^{-4}	18.9	0.23
17	14:29	68	1.25×10^{-3}	11	4.56×10^{-3}	3	8.08×10^{-4}	17.2	0.09
18	11:04	18	1.49×10^{-4}	93	4.89×10^{-3}	2.8	5.55×10^{-4}	25.12	0.09
20	12:14	44	1.05×10^{-3}	13	6.04×10^{-3}	2.3	9.37×10^{-4}	14.8	0.32
21	14:00	64	7.55×10^{-4}	18	3.98×10^{-3}	3.5	1.58×10^{-4}	89.2	0.26
29	13:20	120	4.04×10^{-4}	34	4.96×10^{-3}	2.8	1.24×10^{-4}	113.6	0.15
33	14:40	107	1.48×10^{-4}	94	4.80×10^{-3}	2.9	2.67×10^{-4}	52	0.10
36	10:45	129	9.22×10^{-5}	151	1.58×10^{-3}	8.8	4.95×10^{-4}	28.0	0.09
37	12:05	93	1.30×10^{-4}	107	6.53×10^{-3}	2.1	1.05×10^{-4}	132.3	1.2
38a	13:27	40	1.58×10^{-4}	88	1.12×10^{-3}	12.5	2.52×10^{-4}	55.5	0.66
38b	14:17	85	3.10×10^{-4}	45	4.66×10^{-3}	3	1.25×10^{-4}	111	1.69
38	14:00	112	3.08×10^{-4}	45	4.02×10^{-3}	3.5	1.72×10^{-4}	82	1.8

The mixing times (h^{-1}) derived from K_{PP} (K_{PP} MT) and the calculated VMI for the upper 50 m for each station.

DES index and estimates of vertical mixing

The integrated mean of the DES index over the sampling depth (50 m) was significantly related (Pearson's correlation $r = 0.35$, $n = 15$) with the MLD (Fig. 5A). The MLD varied between 18 and 129 m (Table II). At three stations (18, 20 and 38a), the MLD was shallower than the sampling depth for the XC pigments. The lowest mean DES occurred when the MLD was shallow and the highest mean DES with the deepest MLD. The mean DES was significantly correlated ($P < 0.001$) with the K_G estimates of vertically averaged vertical diffusivity (Fig. 5B), but was not correlated with the K_{PP} estimates (Fig. 5C).

DISCUSSION

By measuring the vertical distribution of the DES in the water column and determining the first-order kinetic equations for the de-epoxidation of Dd to Dt with *in situ* experiments under natural light, it has been possible to estimate the vertical velocity ($1.05 \times 10{-}3$ to $9.22 \times 10{-}5$ m s^{-1}) and mixing times (7–150 h) of algal cells possessing the XC in the open ocean. The values reported here are within the range reported for the coastal Mediterranean (Brunet *et al.*, 2003).

There was no correlation between the DES index and water properties. The highest values of Dd/Chl *a* occurred between Stations 36 and 38, in colder and fresher surface water associated with the Subantarctic Front (SAF) (Uddstrom and Oien, 1999). The phytoplankton species assemblages in these waters during austral autumn are dominated by small-celled nanoflagellates and diatoms (Chang and Gall, 1998). The higher values of Dd are possibly a result of change in species composition with a population consisting of more diatoms, which contain higher cellular concentrations of XC pigments than nanoflagellates and are considered an opportunistic group able to exploit frontal areas such as the SAF (Sakshaug *et al*, 1997). The high concentration of Dd may be a consequence of subnanomolar concentrations of dissolved iron found in the region (Boyd, 2002). Under iron stress, the cellular concentration of Dd in relation to Chl *a* has been shown to increase (Kosakowska *et al*, 2004).

XC activity occurred throughout the study area with Dt present throughout the water column. Given the lower irradiance conditions of autumn, Dt content was

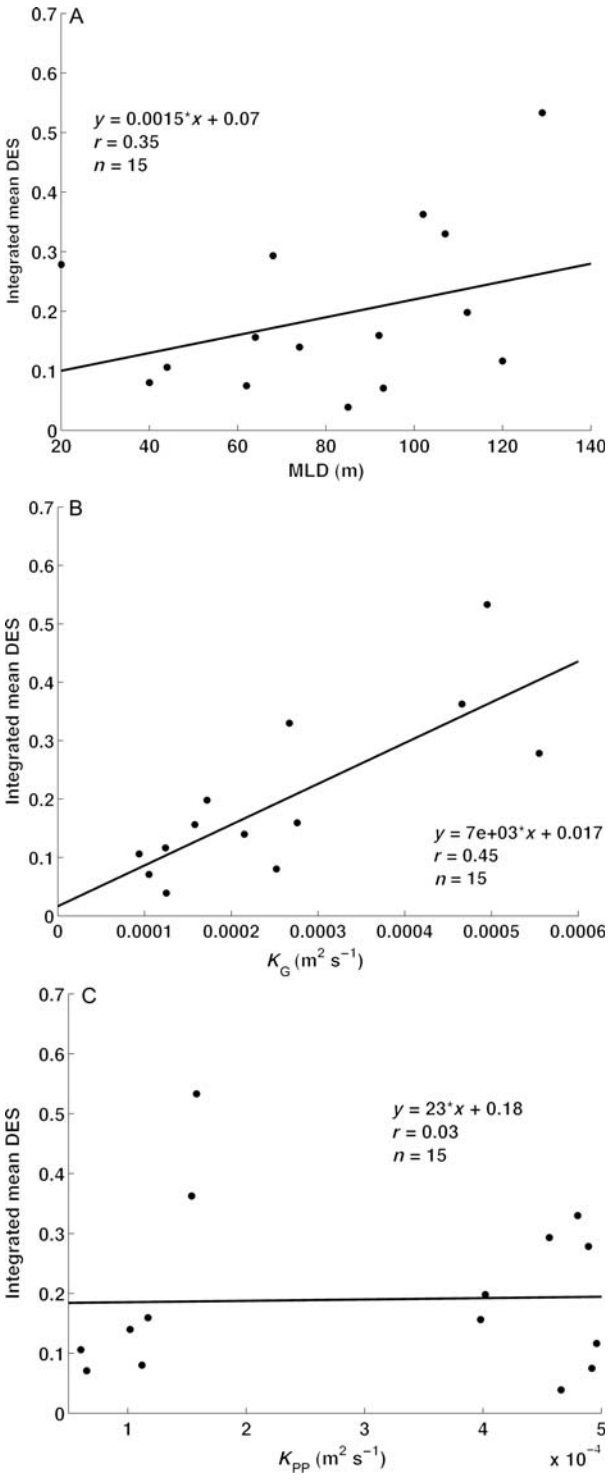

Fig. 5. Relationships between the integrated mean DES and (**A**) mixed layer depth (MLD), (**B**) K_G eddy diffusivity estimate and (**C**) K_{PP} eddy diffusivity estimate.

expected to be low. Southern Ocean phytoplankton are known to be shade adapted and it is possible that the XC is activated under lower irradiance conditions than temperate species. Oceanic diatoms are considered to have lower photoprotective ability compared with coastal diatoms possibly as an adaptation to low iron stress (Strzepek and Harrison, 2004). In our study, the Dt content and DES index suggest the opposite.

The amount of Dt may indicate incomplete epoxidation of Dt back to Dd affecting the DES. The recovery of pigments in the dark or under low light conditions occurs on a much slower time scale. The diel variation in vertical profiles of Dd-cycle pigments in Southern Ocean waters south of Australia have demonstrated that phytoplankton are able to fully adapt to the darkness at all depths (Clementson *et al*, 2001).

Comparison of mixing estimates

To test the hypothesis that the vertical profile of the DES can be used to estimate vertical velocity and mixing times within the surface mixed layer, we applied two independent physical estimates of mixing. Because light decreases exponentially with depth, vertical displacement by eddy diffusion and internal waves results in a phytoplankton cell being exposed to an average light intensity greater than the light intensity at the cell's average depth during the day. K_G which is a measure of vertical diffusivity associated with internal waves was significantly correlated with the DES index ($P < 0.001$) but not with the physical estimate of K_{PP} (Fig. 5B). The RMS of vertical displacement in the deep ocean within one inertial (tidal) period ranges from 7 to 20 m by internal waves to less than 1 m from eddy diffusion (Woods and Wiley, 1972). For algal cells within the euphotic zone, vertical motion by turbulent eddy diffusion (K_{PP}) is unlikely to increase average light intensity in comparison with internal waves (K_G). For eutrophic waters, Lande and Yentsch (Lande and Yentsch, 1988) have shown that internal waves can increase average light intensity on phytoplankton in the lower euphotic zone by 1.65–7.38.

The bathymetry of the study area varies significantly. Stations 14 to 20 are located across the edge of the Pukaki Rise and Stations 21–35 are located across the southern edge of the Bounty Plateau (Fig. 1). Internal waves generated at a shelf such as on the edge of the Pukaki Rise and Bounty Plateau can be tens of metres (Garrett and Munk, 1979), which may contribute to the high K_G values. At Stations 37, 38a, 38b and 38, which were all sampled within the same daylight period and within the same water mass from 0700h to 1600h local time, the relationship between these two estimates is statistically significant (least squares regression $r^2 = 0.70$, $n = 24$, $P < 0.01$). The correlation is less for the other stations which were not sampled within the same

12 h period and within the same water mass. This implies that for short time scales (<12 h) and within similar water mass, the DES index provides (within one order of magnitude) an estimate of averaged vertical velocity representative of the bulk vertical eddy diffusivity generated by internal waves. Consequently, the DES index is potentially a useful biological tracer of the influence of internal waves on the XC cycle.

At some stations (18, 10 and 38a), the MLD was shallower than our sampling depth and at the remaining stations the MLD was deeper than the sampling depth. Without vertical displacement of the algal cells, the DES index should be lower the deeper the MLD as a result of lower integrated PAR. In this study, the DES index increased the deeper the MLD (Fig. 5A) suggesting that vertical displacement has a more significant effect on the DES index than the depth of the MLD.

Conceptual model of the response of the pigment ratio to vertical mixing

The relationship between phytoplankton photoprotection and vertical mixing processes in the surface mixed layer can be interpreted using a simple conceptual model of the DES based on the concept of hysteresis proposed by Cullen and Lewis (Cullen and Lewis, 1988) in which the DES index represents the light history of the sampled phytoplankton. This concept has been successfully applied using a range of photoadaptive parameters (Cullen and Lewis, 1988; Dusenberry, 2000; Oliver *et al*, 2003). The Dd-cycle offers a significant advantage over the other photoadaptive parameters as the light response of the conversion of Dd to Dt occurs rapidly (seconds to minutes), while the reverse conversion from Dt to Dd in the dark or under low light occurs significantly slower (minutes to hours).

The DES index reflects the highest irradiance experienced in their recent light history (seconds to minutes) within the water column. We have assumed that the DES at one depth represents an average of the cells of the natural population within the length scale of the sampling, which in this case is 10 m. If phytoplankton cells are vertically at rest and adapted to the highest irradiance at each depth then the activity of the Dd-cycle will be adapted to the irradiance at that depth and the curve of the index DES will correspond to the curve of the irradiance profile. That is, DES = I, where I = irradiance. If, on the other hand, vertical mixing begins to affect the cell, the relationship of the vertical profile of the DES to the light profile will be disrupted. If the cell is transported faster than the change in the DES with the increasing light field, then the light profile and the profile of the DES index will differ.

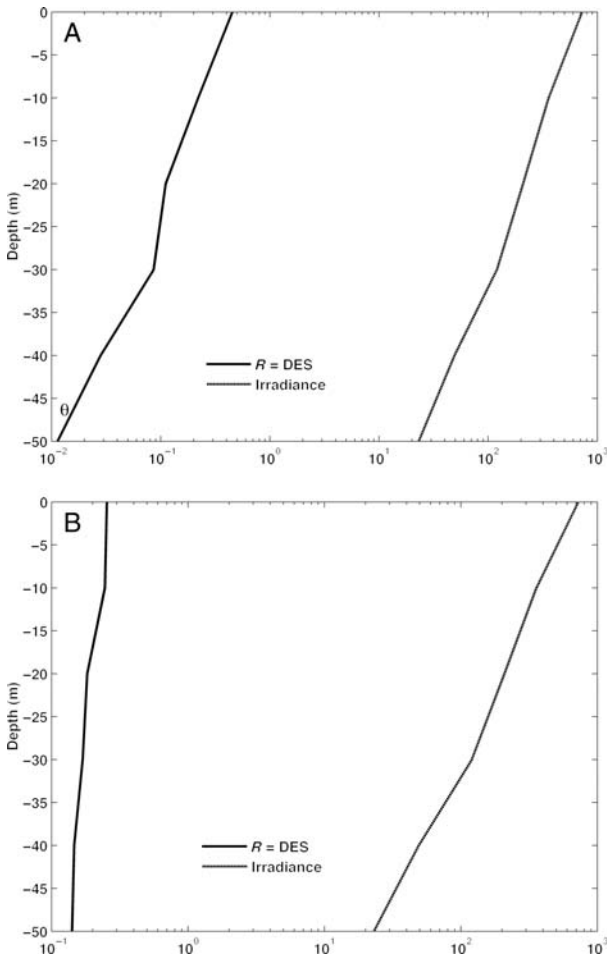

Fig. 6. Conceptual model of the vertical response of the photoprotective ratio DES to the irradiance profile I as a measure of the relative intensity of vertical mixing. The difference in the slope of the DES and I is the relative intensity of vertical mixing which is important in (**B**) but not in (**A**).

The difference between the two curves is then an indication of the relative importance of vertical mixing. The relative difference between the two curves can be shown as a ratio of the slope of the regression between depth and the log of the irradiance profile In *(I)* and the slope of the regression between depth and the log of the photophysiological index In (DES) (Fig. 6). When the photoprotective response of the phytoplankton is at a similar time scale to the change in irradiance then the slope of DES will match the slope of the irradiance profile (Fig. 6A). However, if the cells are being advected vertically at a rate faster than the photoprotective response, then the difference between the two profiles DES and I can be interpreted to indicate vertical motion caused by turbulent mixing and/or sinking (Fig. 6B).

This difference between the slopes of DES and irradiance can be quantified by the ratio of the slope of *DES*

divided by the slope of I. An index which we have termed the bulk vertical mixing index (VMI) can then be estimated for each station:

$$\mathrm{VMI} = \frac{\Delta R - \Delta I}{M} \tag{8}$$

where R is the slope of the index Dt/(Dt + Dt) and I the slope of the irradiance profile, $M = \tan\theta$.

A value of 1 indicates that the time scales of photoprotection and vertical mixing are equal. If the VMI is greater than 1, this indicates the greater relative magnitude of vertical mixing. A VMI less than 1 suggests that either there is insufficient light for the Dd-cycle to be active or that the relative magnitude of photoprotection is less than vertical mixing. It is important to note that the VMI only provides an upper bound of the vertical mixing and/or sinking within the depth profile. At any depth, the natural population of phytoplankton will consist of both sinking and mixing cells. The effects of mixing and sinking cannot be separated and that the value of the ratio at any depth can represent rising cells adapting to the irradiance or cells sinking which have adapted to a higher irradiance.

By providing a quantitative basis of the relative importance of the two opposing processes of vertical mixing and photoprotection, the VMI provides information which is not obvious in either DES index profiles (Fig. 4) or the biological and physical estimates of vertical velocities, eddy diffusivities and mixing times (Table II). In our study, the VMI is significantly related to the integrated mean DES ($P < 0.001$) and the K_G estimates ($P < 0.001$). As such, the VMI index can be used to assess the response of the photoprotective Dd-cycle of phytoplankton to physical changes in the surface mixed layer on the length and time scale of internal waves, but provides no information on the smaller length and time scales of diffusion processes. The low VMI index at Stations 17, 18, 33 and 36 (Fig. 7) strongly suggests that the photoprotective response of the phytoplankton occurs on a faster time scale than vertical mixing indicating that the mixing is slow enough to allow the photoprotective adaptation of phytoplankton in the water column or that there was insufficient irradiance to activate the Dd-cycle. At Stations 37, 38a and 38b, the VMI index is very high showing the importance of vertical mixing over phytoplankton photoprotection. In this case, phytoplankton cells are transported at a faster rate than the rate at which the de-epoxidation of Dd to Dt would normally occur with a change in irradiance without vertical motion. This would suggest that under these conditions, the photoprotective response of the phytoplankton does not match the increase in light intensity caused by rapid vertical motion.

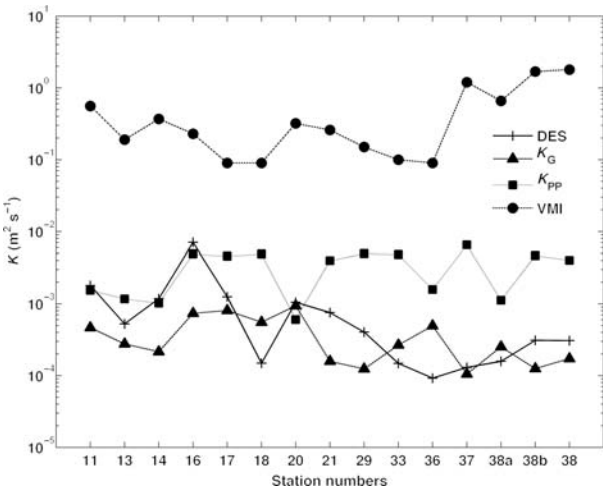

Fig. 7. Vertically averaged vertical velocity (m^2 cm^{-1}) calculated from the DES and eddy diffusivity estimates (K_G and K_{PP}) for the upper 50 m of the surface mixed layer and VMI illustrated for all daytime stations.

In conclusion, the vertical distribution of the DES index together with *in situ* kinetic rate changes can provide useful information on the photoprotective status of Southern Ocean phytoplankton. A comparison between the DES index and physical estimates of vertical displacement suggests that internal waves by increasing the average light intensity result in a higher photoprotective response. By comparing the vertical distribution of the DES with the vertical distribution of light, a simple index (VMI) establishes a relationship between short-term mixing dynamics in the surface mixed layer, irradiance in the euphotic zone and phytoplankton photoprotection. This relationship can potentially provide additional insights into the XC response of shade adapted open ocean phytoplankton to vertical displacements.

ACKNOWLEDGEMENTS

The authors wish to thank the crew of the NIWA research vessel Tangaroa, Matt Walkington for assistance with the ADCP analysis, Karen Bonney and Bev Dickson of Portobello Marine Laboratory for their assistance with HPLC analysis. We gratefully acknowledge two anonymous referees for their suggestions and criticisms, which helped improve the paper.

FUNDING

This study was made possible by University of Otago Division of Science award granted to G.P.G.

REFERENCES

Arsalane, W., Rousseau, B. and Duval, C. (1994) Influence of the pool size of the xanthophyll cycle on the effects of light stress in a diatom: competition between photoprotection and photoinhibition. *Photochem. Photobiol.*, **60**, 237–243.

Bidigare, R. R., Smith, R. C., Baker, K. S. *et al.* (1987) Oceanic primary production estimates from measurements of spectral irradiance and pigment concentrations. *Global Biogeochem. Cycles*, **1**, 171–186.

Boyd, P. W. (2002) Environmental factors controlling phytoplankton processes in the Southern Ocean. *J. Phycol.*, **38**, 844–861.

Brunet, C., Davoult, D. and Casotti, R. (1996) Physiological reactions to a change in light regime in cultured *Skeletonema costatum* (Bacillariophyta): implications to estimation of phytoplankton biomass. *Hydrobiologia*, **333**, 87–94.

Brunet, C., Casotti, R., Arbonne, B. *et al.* (2003) Measured photophysiological parameters used as tools to estimate vertical water movements in the coastal Mediterranean. *J. Plankton Res.*, **25**, 1413–1425.

Brunet, C., Casotti, R., Vantrepotte, V. *et al.* (2006) Picophytoplankton diversity and photophysiology in the Strait of Sicily (Mediterranean Sea) in summer. I. Mesoscale variations. *Aquat. Microb. Ecol.*, **44**, 127–141.

Brunet, C., Casotti, R., Vantrepotte, V. *et al.* (2007) Vertical variability and diel dynamics of picophytoplankton in the Strait of Sicily, Mediterranean Sea, in summer. *Mar. Ecol. Prog. Ser.*, **346**, 15–26.

Brunet, C., Casotti, R. and Vantrepotte, V. (2008) Phytoplankton diel and vertical variability in photobiological responses at a coastal station in the Mediterranean Sea. *J. Plankton Res.*, **30**, 645–654.

Casper-Lindley, C. and Bjorkman, O. (1998) Fluorescence quenching in four unicellular algae with different light-harvesting and xanthophyll-cycle pigments. *Photosynth. Res.*, **56**, 277–289.

Chang, F. H. and Gall, M. (1998) Phytoplankton assemblages and photosynthetic pigments during winter and spring in the Subtropical convergence near New Zealand. *N.Z. J. Mar. Fresh.*, **32**, 515–530.

Cisewski, B., Volker, V. H. and Prandke, H. (2005) Upper-ocean vertical mixing in the Antarctic Polar Front Zone. *Deep-Sea Res. II*, **52**, 1087–1108.

Claustre, H., Kerhervé, P., Marty, J.-C. *et al.* (1994) Phytoplankton photoadaptation related to some frontal physical processes. *J. Mar. Sys.*, **5**, 251–265.

Clementson, L. A., Parslow, J. S., Turnbull, A. R. *et al.* (2001) Optical properties of waters in the Australasian sector of the Southern Ocean. *J. Geophys. Res.*, **106**, 31611–31635.

Cullen, J. J. and Lewis, M. R. (1988) The kinetics of algal photoadaptation in the context of vertical mixing. *J. Plankton Res.*, **10**, 1039–1063.

Dimier, C., Corato, F., Tramontano, F. *et al.* (2007) Photoprotection and xanthophyll activity in three diatoms. *J. Phycol.*, **43**, 937–947.

Dimier, C., Brunet, C., Geider, R. *et al.* (2009a) Growth and photoregulation dynamics of the picoeukaryote *Pelagomonas calcealata* in fluctuating light. *Limnol. Oceanogr.*, **54**, 823–836.

Dimier, C., Giovanni, S., Ferdinando, T. *et al.* (2009b) Comparative ecophysiology of the xanthophyll cycle in six marine phytoplanktonic species. *Protist*, **160**, 397–411.

Dusenberry, J. A. (2000) Steady-state single cell model simulations of photoacclimation in a vertically mixed layer: implications for biological tracer studies and primary productivity. *J. Mar. Sys.*, **24**, 210–220.

Dusenberry, J. A., Olson, R. J. and Chisholm, S. W. (1999) Frequency distributions of phytoplankton single cell fluorescence and vertical mixing in the surface oceans. *Limnol. Oceanogr.*, **44**, 431–435.

Falkowski, P. G. (1983) Light-shade adaptation and vertical mixing of marine phytoplankton: a comparative study. *J. Mar. Res.*, **41**, 215–237.

Franks, P. J. S. and Marra, J. (1994) A simple new formulation for phytoplankton photoresponse and an application in a wind-driven mixed-layer model. *Mar. Ecol. Prog. Ser.*, **111**, 143–153.

Fujiki, T. and Taguchi, S. (2002) Variability in chlorophyll a specific absorption coefficient in marine phytoplankton as a function of cell size and irradiance. *J. Plankton Res.*, **24**, 859–874.

Garrett, C. J. R. and Munk, W. H. (1979) Internal waves in the oceans. *Annu. Rev. Fluid Mech.*, **11**, 339–369.

Gregg, M. C. (1989) Scaling turbulent dissipation in the thermocline. *J. Geophys. Res.*, **94**, 9686–9698.

Jeffrey, S. W. and Vesk, M. (1997) Introduction to marine phytoplankton and their pigment signatures. In Jeffrey, S. W., Mantoura, R. F. C. and Wright, S. W. (eds), *Phytoplankton Pigments in Oceanography.* UNESCO Publishing, Paris, pp. 37–84.

Kashino, Y., Kudoh, S., Hayashi, Y. *et al.* (2002) Strategies of phytoplankton to perform effective photosynthesis in the North Water. *Deep-Sea Res. II*, **49**, 5049–5061.

Kosakowska, A., Lewandowska, J., Stón, J. and Burkiewicz, K. (2004) Qualitative and quantitative composition of pigments in *Phaedactylum tricornutum* (Bacillariophyceae) stressed by iron. *Biometals*, **17**, 45–52.

Kruskopf, M. and Flynn, K. J. (2006) Chlorophyll content and fluorescence responses cannot be used to gauge reliably phytoplankton biomass, nutrient status or growth rate. *New Phytol.*, **169**, 525–536.

Lande, R. and Yentsch, C. S. (1988) Internal waves, primary production and the compensation depth of marine phytoplankton. *J. Plankton Res.*, **10**, 565–571.

Lavaud, J., Rousseau, B. and Etienne, L. (2002a) In diatoms, a trans thylakoidal proton gradient alone is not sufficient for non-photochemical fluorescence quenching. *FEBS Lett.*, **523**, 1163–1166.

Lavaud, J., Rousseau, B., van Gorkom, H. *et al.* (2002b) Influence of the diadinoxanthin pool size on photoprotection in the marine planktonic diatom *Phaeodactylum tricornutum.*. *Plant Physiol.*, **129**, 1398–1406.

Lavaud, J., Rousseau, B. and Etienne, L. (2004) General features of photoprotection by energy dissipation in planktonic diatoms (Bacillariophyceae). *J. Phycol.*, **40**, 130–137.

Lavaud, J., Strzepeck, R. F. and Kroth, P. G. (2007) Photoprotection capacity differs among diatoms: possible consequences on the spatial distribution of diatoms related to fluctuations in the underwater light climate. *Limnol. Oceanogr.*, **52**, 1188–1194.

Law, C. S., Abraham, E. R., Watson, A. J. *et al.* (2003) Vertical eddy diffusion and nutrient supply to the surface mixed layer of the Antarctic Circumpolar Current. *J. Geophys. Res.*, **108**, No. C8, 3272, doi: 10.1029/2002JC001604.

MacIntyre, H. L. and Geider, R. J. (1996) Regulation of Rubisco activity and its potential effect on photosynthesis during mixing in a turbid estuary. *Mar. Ecol. Prog. Ser.*, **44**, 247–264.

Mantoura, R. F. C., Wright, S. W., Jeffrey, S. W. *et al.* (1997) Filtration and storage of pigments from microalgae. In Jeffrey, S. W.,

Mantoura, R. F. C. and Wright, S. W. (eds), *Phytoplankton Pigments in Oceanography*. UNESCO Publishing, Paris, pp. 283–305.

Moline, M. A. (1998) Photoadaptive response during the development of a coastal Antarctic diatom bloom and relationship to water column stability. *Limnol. Oceanogr.*, **43**, 146–153.

Morris, M., Stanton, B. and Neil, H. (2001) Subantarctic oceanography around New Zealand: preliminary results from an ongoing survey. *N.Z. J. Mar. Fresh.*, **35**, 499–519.

Olaizola, M. and Yamamoto, H. Y. (1994) Short-term response of the DD-cycle and fluorescence yield to high irradiance in *Chaetoceros muelleri* (Bacillariophyceae). *J. Phycol.*, **30**, 606–612.

Olaizola, M., Bienfang, P. K. and Zieman, D. A. (1992) Pigment analysis of phytoplankton during a subarctic spring bloom: xanthophyll cycling. *J. Exp. Mar. Biol. Ecol.*, **158**, 59–74.

Olaizola, M., la Roche, J., Kolber, Z. *et al.* (1994) Non-photochemical fluorescence quenching and the diadinoxanthin cycle in marine diatom. *Photosynth. Res.*, **41**, 357–370.

Oliver, R. L., Whittington, J., Lorenz, Z. *et al.* (2003) The influence of vertical mixing on the photoinhibition of variable chlorophyll *a* fluorescence and its inclusion in a model of phytoplankton photosynthesis. *J. Plankton Res.*, **25**, 1107–1129.

Pacanowski, R. C. and Philander, S. G. H. (1981) Parameterization of vertical mixing in numerical models of tropical oceans. *J. Phys. Oceanogr.*, **11**, 1443–1451.

Sakshaug, E., Bricaud, A., Dandonneau, Y. *et al.* (1997) Parameters of photosynthesis: definitions, theory and interpretation of results. *J. Plankton Res.*, **19**, 1637–1670.

Staehr, P. A., Henriksen, P. and Markager, S. (2002) Photoacclimation of four marine phytoplankton species to irradiance and nutrient availability. *Mar. Ecol. Prog. Ser.*, **237**, 47–59.

Strzepek, R. F. and Harrison, P. J. (2004) Photosynthetic architecture differes in coastal and oceanic diatoms. *Nature*, **431**, 689–692.

Therriault, J.-C., Booth, D., Legendre, L. *et al.* (1990) Phytoplankton photoadaptation to vertical excursion as estimated by an in vivo fluorescence ratio. *Mar. Ecol. Prog. Ser.*, **60**, 97–111.

Uddstrom, M. J. and Oien, N. A. (1999) On the use of high-resolution satellite data to describe the spatial and temporal variability of sea surface temperatures in the New Zealand region. *J. Geophys. Res.*, **104**, 20729–20751.

Walkington, M. (2003) NIWA Voyage Report TAN0307 Subantarctic 5. *NIWA Internal Report*. National Institute of Water and Atmosphere, Wellington, New Zealand.

Woods, J. D. and Wiley, R. L. (1972) Billow turbulence and ocean microstructure. *Deep-Sea Res.*, **19**, 87–121.

Wright, S. W. and Mantoura, R. F. C. (1997) Guidelines for collection and pigment analysis of field samples. In Jeffrey, S. W., Mantoura, R. F. C. and Wright, S. W. (eds), *Phytoplankton Pigments in Oceanography*. UNESCO Publishing, Paris, pp. 429–445.

Zapata, M., Rodríguez, F. and Garrido, J. L. (2000) Separation of chlorophylls and carotenoids from marine phytoplankton: a new HPLC method using a reversed phase C_8 column and pyridine-containing mobile phases. *Mar. Ecol. Prog. Ser.*, **195**, 29–45.